



**HAL**  
open science

# NDIPhos as a platform for chiral supramolecular ligands in rhodium-catalyzed enantioselective hydrogenation

Guillaume Force, Robert J Mayer, Marie Vayer, David Lebœuf

## ► To cite this version:

Guillaume Force, Robert J Mayer, Marie Vayer, David Lebœuf. NDIPhos as a platform for chiral supramolecular ligands in rhodium-catalyzed enantioselective hydrogenation. *Chemical Communications*, 2023, 59 (41), pp.6231 - 6234. 10.1039/d3cc00695f. hal-04762389

**HAL Id: hal-04762389**

**<https://hal.science/hal-04762389v1>**

Submitted on 31 Oct 2024

**HAL** is a multi-disciplinary open access archive for the deposit and dissemination of scientific research documents, whether they are published or not. The documents may come from teaching and research institutions in France or abroad, or from public or private research centers.

L'archive ouverte pluridisciplinaire **HAL**, est destinée au dépôt et à la diffusion de documents scientifiques de niveau recherche, publiés ou non, émanant des établissements d'enseignement et de recherche français ou étrangers, des laboratoires publics ou privés.



Distributed under a Creative Commons Attribution - NonCommercial - NoDerivatives 4.0  
International License



Cite this: *Chem. Commun.*, 2023, 59, 6231

Received 14th February 2023,  
Accepted 25th April 2023

DOI: 10.1039/d3cc00695f

rsc.li/chemcomm

# NDIPhos as a platform for chiral supramolecular ligands in rhodium-catalyzed enantioselective hydrogenation†

Guillaume Force,<sup>a</sup> Robert J. Mayer,<sup>id</sup> Marie Vayer,<sup>id</sup> and David Lebœuf<sup>id</sup>\*

Chiral naphthalene diimide ligands (NDIPhos) were exploited in rhodium-catalyzed enantioselective hydrogenation. The key feature of these ligands is their ability to self-assemble *via*  $\pi$ - $\pi$  interactions to mimic bidentate ligands, offering a complementary method to traditional supramolecular strategies. This concept was further substantiated by computations with the composite electronic-structure method  $r^2$ SCAN-3c.

Transition metal catalysis is instrumental to our daily life. It is indeed crucial to the production of high value-added molecules that are prevalent in our food, drugs, cosmetics, and agrochemicals. Two major breakthroughs in transition metal catalysis were related to the discovery of (1) bidentate ligands that form metal complexes of well-defined geometry through the chelation of the metal center for better control of the selectivity<sup>1</sup> – currently the main players in catalysis – and (2) cationic organometallic complexes displaying weakly coordinating anions that readily ease the encounter with the substrates to accelerate transformations under milder reaction conditions.<sup>2</sup> In search of new reactivity, synthetic chemists have designed hundreds of new bidentate ligands and thousands of new cationic complexes. However, these processes can become laborious as screening various catalysts can be hampered by limited access to libraries of structurally diverse ligands. This is particularly the case for bidentate ligands, whose preparation can be both time-consuming and expensive.

To overcome these drawbacks, the self-assembly of monodentate ligands *via* non-covalent interactions has emerged as a powerful strategy to mimic bidentate ligands around the metal center.<sup>3</sup> This approach grants direct access to a large combinatorial library for catalysts through the straightforward preparation of monodentate ligands. Existing supramolecular approaches in

transition metal asymmetric catalysis mostly rely on hydrogen bonding, coordination to a metal center, and electrostatic interactions to provide well-defined homo- and heterobidentate ligand–metal complexes as illustrated by the groups of Breit,<sup>4</sup> Reek,<sup>5</sup> Gennari,<sup>6</sup> Nishibayashi,<sup>7</sup> Takacs,<sup>8</sup> van Leeuwen,<sup>9</sup> Fan,<sup>10</sup> and Vidal-Ferran (Fig. 1).<sup>11</sup> However, in several cases, the incorporation of selective recognition units makes the synthesis of such assemblies more elaborate and costly than intended. Additionally, these non-covalent interactions can be disrupted by highly polar functional groups, which can drastically limit their efficiency and range of applications.

In this context, we wondered if we could develop a supramolecular approach that retains the benefits of self-assembled ligands but eliminates their negative aspects. Hence, our attention was drawn to  $\pi$ - $\pi$  interactions that, if sufficiently strong, are less prone to be impacted by polar functionalities. To date, the use of  $\pi$ -stacking for the design of self-assembled ligands remains underexplored in transition metal catalysis unless it is combined with other non-covalent interactions.<sup>12</sup>

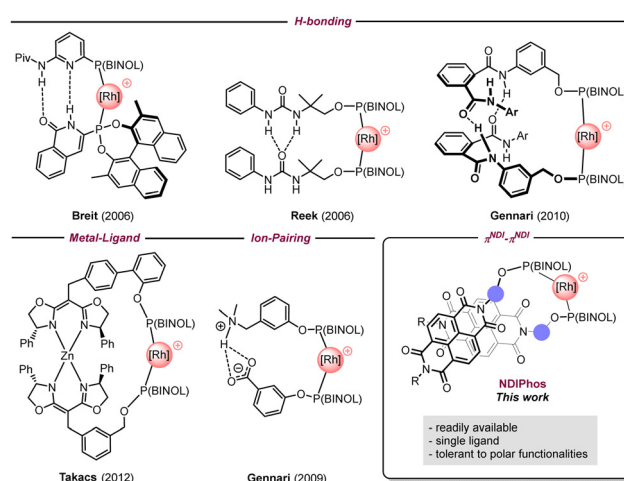


Fig. 1 Selected examples of supramolecular self-assembled ligands for transition metal catalysis.

<sup>a</sup> Institut de Chimie Moléculaire et des Matériaux d'Orsay (ICMMO), CNRS UMR 8182, Université Paris-Saclay, Orsay 91405, France

<sup>b</sup> Institut de Science et d'Ingénierie Supramoléculaires (ISIS), CNRS UMR 7006, Université de Strasbourg, Strasbourg 67000, France. E-mail: dlebœuf@unistra.fr

† Electronic supplementary information (ESI) available. See DOI: <https://doi.org/10.1039/d3cc00695f>



Attempts have been made by the group of Gennari to use  $\pi$ - $\pi$  interactions between perfluoro phenyls and electron-rich arenes,<sup>13</sup> but without much success. The reason behind this result is likely the weakness of such interactions in solution. To overcome this issue, we assumed that naphthalene diimides (NDIs) that are well known for their ability to strongly self-assemble through  $\pi$ -stacking, could represent a viable solution to obtain stable formal bidentate ligands.<sup>14</sup> While the use of NDIs has become increasingly popular in materials sciences, they have only been featured in a few applications in catalysis, mainly in  $\pi$ -anion catalysis by the group of Matile.<sup>15</sup> Therefore, developing such an approach could expand the range of applications of NDIs in synthesis. Here we describe our efforts regarding the preparation of chiral self-assembled NDIPhos-based catalysts and their application to enantioselective hydrogenations as a proof of concept.

To validate our hypothesis regarding the capacity of NDI-derived ligands to undergo the anticipated self-assembly, we initially performed a computational analysis of the adduct formation of the model ligand **L** and  $\text{Rh}(\text{COD})_2^+$  by adapting a protocol from Grimme and co-workers for the study of non-covalent interactions (Fig. 2).<sup>16</sup> This procedure relies on the composite electronic-structure method  $r^2\text{SCAN-3c}$ , which includes the D4-dispersion correction and a geometrical counterpoise correction.<sup>17</sup> It was shown that this functional achieves comparable results to classical hybrid-DFT methods, but only with a fraction of the computational cost, making it particularly suitable for large systems like ours. After a conformational search at the GFN2-xTB(ALPB =  $\text{CH}_2\text{Cl}_2$ ) level with the CREST program,<sup>18</sup> structures were optimized at the  $r^2\text{SCAN-3c}(\text{SMD} = \text{CH}_2\text{Cl}_2)$  level of theory within ORCA.<sup>19,20</sup> Thermochemical corrections were obtained using the single-point Hessian (SPH) approach at the GFN2-xTB(ALPB =  $\text{CH}_2\text{Cl}_2$ ) level with the  $r^2\text{SCAN-3c}(\text{SMD} = \text{CH}_2\text{Cl}_2)$ -optimized structures as input. On the energetically lowest conformers obtained in this way, additional numerical frequency calculations were performed using the  $r^2\text{SCAN-3c}(\text{SMD} = \text{CH}_2\text{Cl}_2)$  method.<sup>21</sup> For further verification of the methods, control

computations were performed at the  $(\text{SMD} = \text{CH}_2\text{Cl}_2)/\text{M06-L}/\text{def2-TZVP}$  level. As evidenced by an analysis of the non-covalent interactions (NCIs),<sup>22</sup> the model ligand **L** already features intramolecular  $\pi$ -stacking interactions between the NDI moiety and the naphthyl group. Dimerization of **L** to  $(\text{L})_2$  was computed to be exergonic at the  $r^2\text{SCAN-3c}(\text{SMD} = \text{CH}_2\text{Cl}_2)$  level ( $\Delta G = -10.0/-15.6 \text{ kJ mol}^{-1}$ ) but slightly endergonic at the  $(\text{SMD} = \text{CH}_2\text{Cl}_2)/\text{M06-L}/\text{def2-TZVP}$  level ( $\Delta G = +9.4 \text{ kJ mol}^{-1}$ ). The resulting structure features extensive  $\pi$ - $\pi$  and  $\text{CH}-\pi$  interactions between the NDI and the naphthyl units. In  $(\text{L})_2$ , both phosphorus atoms are oriented in a way that allows  $(\text{L})_2$  to act as a bidentate ligand to yield a *cis*-phosphite rhodium complex. The binding of  $\text{Rh}(\text{COD})^+$  at  $(\text{L})_2$  was computed to be highly favorable with all methods ( $\Delta G = -81.8/-90.6/-98.7 \text{ kJ mol}^{-1}$ ) and results in only insignificant structural changes of the  $(\text{L})_2$  fragment, thereby retaining the intramolecular interactions, notably the  $\pi$ -stacking. In contrast, the binding of  $\text{Rh}(\text{cod})^+$  at the ligand **L** itself is computed to be less favored ( $\Delta G = -7.4/+0.2/-22.8 \text{ kJ mol}^{-1}$ ). While one carbonyl group of the NDI allows **L** to act as a bidentate ligand along with the phosphorus atom, this ligand is unlikely a good ligand to favor the formation of such a complex. The weak binding of **L** with  $\text{Rh}(\text{cod})^+$  is not surprising as only minor intramolecular interactions between the COD ligand and one of the aryl rings of **L** are retained in the  $\text{Rh}(\text{COD})(\text{L})^+$  adduct. In parallel, we recorded the  $^{31}\text{P}$  NMR spectra of the mixture of  $[\text{Rh}(\text{COD})_2]\text{OTf}$  and **L1** (ratio 1:2 and ratio 1:1) in  $\text{CD}_2\text{Cl}_2$ . Here, the methyl group of **L** was replaced by an *n*-pentyl group to improve the solubility of the corresponding ligand. Both spectra display a doublet at 120.5 ppm with  $^1J_{\text{P,Rh}} = 259.4 \text{ Hz}$ , which is consistent with the two phosphites coordinating to the rhodium center in a *cis*-fashion (see ESI† for details), while the formation of  $[\text{Rh}(\text{COD})\text{L1}]\text{OTf}$  was not observed.

Encouraged by the computational analysis that indicates the defined binding of  $\text{Rh}^+$  in the pre-associated  $(\text{L})_2$  system, we started to evaluate the potential of chiral ligand **L1** in the Rh-catalyzed enantioselective hydrogenation of methyl (*Z*)-2-acetamido-3-phenylacrylate at room temperature under 20 atm of  $\text{H}_2$  for 24 h (Table 1). Using  $[\text{Rh}(\text{COD})(\text{MeCN})_2]\text{BF}_4$  as a

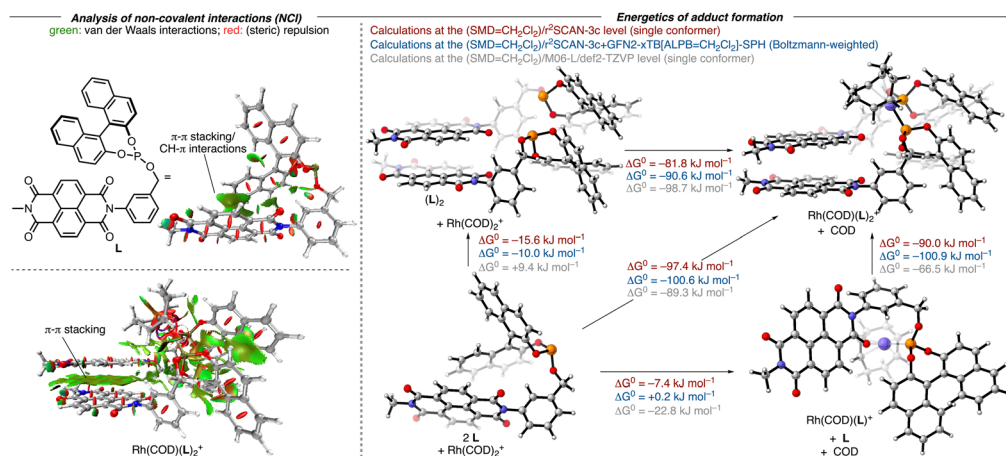
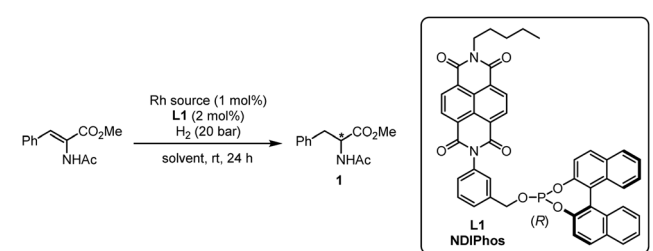


Fig. 2 Left: NCI analysis of the structures at the  $(\text{SMD} = \text{CH}_2\text{Cl}_2)/r^2\text{SCAN-3c}$  level. Right: Geometries of the most favorable conformers for each species optimized at the  $(\text{SMD} = \text{CH}_2\text{Cl}_2)/r^2\text{SCAN-3c}$  and  $(\text{SMD} = \text{CH}_2\text{Cl}_2)/\text{M06-L}/\text{def2-TZVP}$  levels and associated Gibbs free energies for complex formation calculated in three different ways.



Table 1 Optimization of the reaction conditions with **L1**<sup>a</sup>


Entry	Catalyst	Solvent	Conversion <sup>b</sup> (%)	ee <sup>c</sup> (%) abs. config. <sup>d</sup>
1	[Rh(cod)(MeCN) <sub>2</sub> ]BF <sub>4</sub>	CH <sub>2</sub> Cl <sub>2</sub>	> 99	87, <i>S</i>
2	[Rh(cod)(MeCN) <sub>2</sub> ]BF <sub>4</sub>	Toluene	> 99	71, <i>S</i>
3	[Rh(cod)(MeCN) <sub>2</sub> ]BF <sub>4</sub>	Benzene	> 99	80, <i>S</i>
4	[Rh(cod)(MeCN) <sub>2</sub> ]BF <sub>4</sub>	PhNO <sub>2</sub>	> 99	93, <i>S</i>
5	[Rh(cod)(MeCN) <sub>2</sub> ]BF <sub>4</sub>	PhBr	> 99	92, <i>S</i>
6	[Rh(cod)(MeCN) <sub>2</sub> ]BF <sub>4</sub>	1,4-Dioxane	> 99	35, <i>S</i>
7	[Rh(cod)(MeCN) <sub>2</sub> ]BF <sub>4</sub>	MeNO <sub>2</sub>	< 5	—
8	[Rh(cod)(MeCN) <sub>2</sub> ]BF <sub>4</sub>	MeOH	> 99	9, <i>S</i>
9	[Rh(cod)(MeCN) <sub>2</sub> ]BF <sub>4</sub>	CH <sub>2</sub> Cl <sub>2</sub> /PhNO <sub>2</sub>	> 99	95, <i>S</i>
10	[Rh(COD) <sub>2</sub> ]OTf	CH <sub>2</sub> Cl <sub>2</sub> /PhNO <sub>2</sub>	> 99	96, <i>S</i>
11	[Rh(COD) <sub>2</sub> ]SbF <sub>6</sub>	CH <sub>2</sub> Cl <sub>2</sub> /PhNO <sub>2</sub>	> 99	96, <i>S</i>
12 <sup>e</sup>	[Rh(COD) <sub>2</sub> ]SbF <sub>6</sub>	CH <sub>2</sub> Cl <sub>2</sub> /PhNO <sub>2</sub>	> 99	97, <i>S</i>
13	[Rh(COD) <sub>2</sub> ]BARF	CH <sub>2</sub> Cl <sub>2</sub> /PhNO <sub>2</sub>	> 99	96, <i>S</i>

<sup>a</sup> Reaction conditions: substrate/ligand/catalyst = 100:2:1, solvent *c* = 0.13 M, and *T* = 25 °C. <sup>b</sup> Determined by <sup>1</sup>H NMR. <sup>c</sup> Determined by HPLC using a chiral column Daicel Chiralpak IA. <sup>d</sup> Assignment based on comparison with ref. 21. <sup>e</sup> Reaction at 0 °C.

rhodium source (1 mol%), we first investigated the influence of the solvent on the reactivity (entries 1–9). Except for nitromethane, all rhodium complexes were catalytically active with the enantiomeric excesses ranging from 9 to 93%. Here, the best result was obtained with nitrobenzene as a solvent. Interestingly, such a positive effect of nitrobenzene on the reactivity of NDI was already observed by the group of Matile in enantioselective  $\pi$ -anion catalysis.<sup>15c</sup> Based on their observations, a plausible explanation is that an electron-deficient arene might increase the electron-deficiency of the NDI, reinforcing the  $\pi$ - $\pi$  interaction between the NDI units. Of note, the amount of nitrobenzene could be reduced by using a mixture of CH<sub>2</sub>Cl<sub>2</sub>/PhNO<sub>2</sub> (10:1), affording the product with 95% ee (entry 9). Other cationic rhodium sources were also tested and overall produced comparable results (entries 10–13). Reducing the reaction temperature to 0 °C allowed us to slightly improve the enantiomeric excess to 97% (entry 12).

We then compared the reactivity and efficiency of **L1** with other ligands incorporating electron-deficient aromatic scaffolds (Fig. 3). In particular, ligand **L2**, which has a similar structure to the BenzaPhos ligands developed by Gennari,<sup>23</sup> provided the highest enantiomeric excess (ee 98%). Tetrafluorophthalimido-derived ligand **L3** also proved efficient in the transformation (ee 96%). In this case, analogous computations still indicated a well-defined behavior of a pre-associated bidentate ligand for rhodium. However,

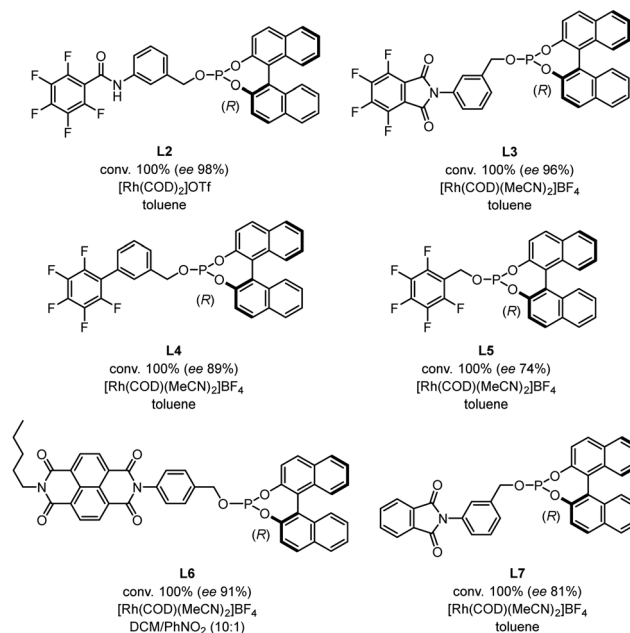


Fig. 3 Comparison with other electron-deficient ligands.

this pre-association is energetically less favored and not as defined as with **L1** (see Fig. S2 for details, ESI<sup>†</sup>). Of note, switching the position of the phosphite moiety from the *meta* to *para* position in **L1** (**L6**) led to a slight decrease of the enantiomeric excess (ee 91%). In the same vein, a drop of the enantiomeric excess (ee 81%) was observed by removing fluorine from **L3**, which might be attributed to the fact that the  $\pi$ -stacking is not possible anymore. Other ligands were also tested but did not afford enantiomeric excesses superior to 90%.

Lastly, we explored the synthetic potential of **L1** with various substrates (Fig. 4), using **L2** and **L3** as references. In the case of classic substrates such as methyl 2-acetamidoacrylate, dimethyl itaconate, and *N*-(3,4-dihydronaphthalen-1-yl)acetamide, all the ligands provided fairly similar results for products 2–4. On the other hand, in the case of 2-acetamidoacrylic acid, we observed significant differences as **L1** afforded 89% ee for 5, while **L2** gave 5% ee, and **L3** gave 37% ee. This clearly demonstrates that in the case of a ligand prone to H-bonding coordination such as

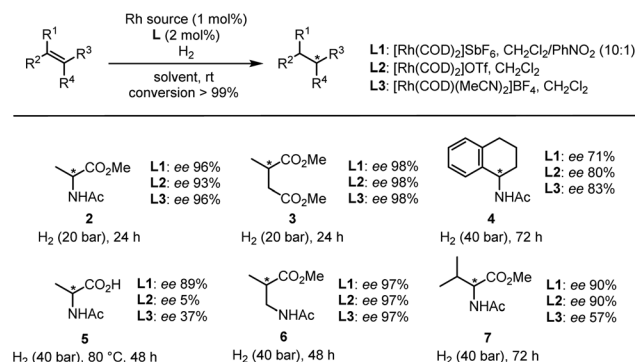


Fig. 4 Scope for the rhodium-catalyzed enantioselective hydrogenation.



**L2**, the presence of a highly polar functional group such as a carboxylic acid is detrimental to the selectivity of the reaction. In addition, if the  $\pi$ -stacking interaction is not strong enough, the reaction becomes less selective as shown by **L3**. **L1** also proved highly selective when a spacer was added (**6**) and when a tetrasubstituted substrate was used (**7**).

In conclusion, we described a new class of self-assembled bidentate NDI-derived ligands featuring  $\pi$ - $\pi$  interactions, which were successfully used in rhodium-catalyzed enantioselective hydrogenation of diverse substrates. The catalysts incorporating this NDIPhos ligand were generally highly selective, notably in the presence of polar functionalities such as carboxylic acids. Our current efforts are dedicated to the improvement of their design to expand their range of applications.

This work was supported by the ANR (ANR-16-CE07-0022, funding for G. F.) and the Interdisciplinary Thematic Institute ITI-CSC via the IdEx Unistra (ANR-10-IDEX-0002, funding for M. V.) within the program Investissement d'Avenir. R. J. M. thanks the Deutsche Forschungsgemeinschaft (DFG, German Research Foundation) for the fellowship (MA 9687/1-1). Computations were performed at the High Performance Computing Center of the University of Strasbourg. Part of the computing resources was funded by the Equipex Equip@Meso project (Programme Investissements d'Avenir) and the CPER Alsacalcul/Big Data. D. L. thanks the CNRS. D. L. thanks Pr. Vincent Gandon and Dr Emmanuelle Schulz for useful discussions. The authors thank Emilie Kolodziej for her help with the HPLC and GC analyses.

## Conflicts of interest

There are no conflicts to declare.

## Notes and references

- (a) T. P. Dang and H. B. Kagan, *J. Chem. Soc. D*, 1971, 481; (b) W. S. Knowles, M. J. Sabacky, B. D. Vineyard and D. J. Weinkauff, *J. Am. Chem. Soc.*, 1975, **97**, 2567; (c) A. Miyashita, A. Yasuda, H. Takaya, K. Toriumi, T. Ito, T. Souchi and R. Noyori, *J. Am. Chem. Soc.*, 1980, **102**, 7932.
- (a) J. A. Osborn and R. R. Schrock, *J. Am. Chem. Soc.*, 1971, **93**, 2397; (b) J. A. Osborn and R. R. Schrock, *J. Am. Chem. Soc.*, 1976, **98**, 4450.
- For selected reviews on supramolecular catalysis, see: (a) J. Meeuwissen and J. N. H. Reek, *Nat. Chem.*, 2010, **2**, 615; (b) M. Raynal, P. Ballester, A. Vidal-Ferran and P. W. N. M. van Leeuwen, *Chem. Soc. Rev.*, 2014, **43**, 1660; (c) C. J. Brown, F. D. Toste, R. G. Bergman and K. N. Raymond, *Chem. Rev.*, 2015, **115**, 3012; (d) J. N. H. Reek, B. de Bruin, S. Pullen, T. J. Mooibroek, A. M. Kluwer and X. Caumes, *Chem. Rev.*, 2022, **22**, 12308; (e) *Supramolecular Catalysis*, ed. P. W. N. M. van Leeuwen and M. Raynal, Wiley-VCH, Weinheim, 2022.
- (a) M. Weis, C. Waloch, W. Seiche and B. Breit, *J. Am. Chem. Soc.*, 2006, **128**, 4188; (b) A. C. Laungani, J. M. Slaterry, I. Krossing and B. Breit, *Chem. – Eur. J.*, 2008, **14**, 4488; (c) J. Wieland and B. Breit, *Nat. Chem.*, 2010, **2**, 832.
- (a) X.-B. Jiang, L. Lefort, P. E. Goudriaan, A. H. M. de Vries, P. W. N. M. van Leeuwen, J. G. de Vries and J. N. H. Reek, *Angew. Chem., Int. Ed.*, 2006, **45**, 1223; (b) A. J. Sandee, A. M. van der Burg and J. N. H. Reek, *Chem. Commun.*, 2007, 864; (c) P.-A. R. Breuil, F. W. Patureau and J. N. H. Reek, *Angew. Chem., Int. Ed.*, 2009, **48**, 2162.
- (a) L. Pignataro, S. Carboni, M. Civera, R. Colombo, U. Piarulli and C. Gennari, *Angew. Chem., Int. Ed.*, 2010, **49**, 6633; (b) L. Pignataro, B. Lynikaite, J. Cvengroš, M. Marchini, U. Piarulli and C. Gennari, *Eur. J. Org. Chem.*, 2009, 2539.
- G. Hattori, T. Hori, Y. Miyake and Y. Nishibayashi, *J. Am. Chem. Soc.*, 2007, **129**, 12930.
- N. C. Thacker, S. A. Moteki and J. M. Takacs, *ACS Catal.*, 2012, **2**, 2743.
- P. W. N. M. van Leeuwen, D. Rivillo, M. Raynal and Z. Freixa, *J. Am. Chem. Soc.*, 2011, **133**, 18562.
- Y. Li, B. Ma, Y. He, F. Zhang and Q.-H. Fan, *Chem. – Asian J.*, 2010, **5**, 2454.
- I. Mon, D. A. Jose and A. Vidal-Ferran, *Chem. – Eur. J.*, 2013, **19**, 2720.
- (a) A. C. Laugani and B. Breit, *Chem. Commun.*, 2008, 844; (b) M. Raynal, F. Portier, P. W. N. M. van Leeuwen and L. Bouteiller, *J. Am. Chem. Soc.*, 2013, **135**, 17687.
- B. Lynikaite, J. Cvengroš, U. Piarulli and C. Gennari, *Tetrahedron Lett.*, 2008, **49**, 755.
- For recent reviews, see: (a) M. Al Kobaisi, S. V. Bhosale, K. Latham, A. M. Raynor and S. V. Bhosale, *Chem. Rev.*, 2016, **116**, 11685; (b) Y. Zhao, Y. Cotelte, L. Liu, J. Lopez-Andarias, A.-B. Bornhof, M. Akamatsu, N. Sakai and S. Matile, *Acc. Chem. Res.*, 2018, **51**, 2255; (c) S. V. Bhosale, M. Al Kobaisi, R. W. Jadhav, P. P. Morajkar, L. A. Jones and S. George, *Chem. Soc. Rev.*, 2021, **50**, 9845.
- For selected examples, see: (a) Y. Zhao, Y. Cotelte, A.-J. Avestro, N. Sakai and S. Matile, *J. Am. Chem. Soc.*, 2015, **137**, 11582; (b) Y. Cotelte, S. Benz, A.-J. Avestro, T. R. Ward, N. Sakai and S. Matile, *Angew. Chem., Int. Ed.*, 2016, **55**, 4275; (c) L. Liu, Y. Cotelte, A.-J. Avestro, N. Sakai and S. Matile, *J. Am. Chem. Soc.*, 2016, **138**, 7876; (d) L. Liu, Y. Cotelte, J. Klehr, N. Sakai, T. R. Ward and S. Matile, *Chem. Sci.*, 2017, **8**, 3770; (e) L. Liu, Y. Cotelte, A.-B. Bornhof, C. Besnard, N. Sakai and S. Matile, *Angew. Chem., Int. Ed.*, 2017, **56**, 13066; (f) M. Paraja and S. Matile, *Angew. Chem., Int. Ed.*, 2020, **59**, 6273.
- (a) M. Bursch, J.-M. Mewes, A. Hansen and S. Grimme, *Angew. Chem., Int. Ed.*, 2022, **61**, e202205735; (b) J. Gorges, S. Grimme and A. Hansen, *Phys. Chem. Chem. Phys.*, 2022, **24**, 28831–28843.
- S. Grimme, A. Hansen, S. Ehlert and J.-M. Mewes, *J. Chem. Phys.*, 2021, **154**, 064103.
- (a) P. Pracht, F. Bohle and S. Grimme, *Phys. Chem. Chem. Phys.*, 2020, **22**, 7169; (b) C. Bannwarth, S. Ehlert and S. Grimme, *J. Chem. Theory Comput.*, 2019, **15**, 1652; (c) S. Ehlert, M. Stahn, S. Spicher and S. Grimme, *J. Chem. Theory Comput.*, 2021, **17**, 4250.
- F. Neese, *Wiley Interdiscip. Rev.: Comput. Mol. Sci.*, 2022, e1606.
- A. V. Marenich, C. J. Cramer and D. G. Truhlar, *J. Chem. Theory Comput.*, 2013, **9**, 609.
- S. Spicher and S. Grimme, *J. Chem. Theory Comput.*, 2021, **17**, 1701.
- (a) E. R. Johnson, S. Keinan, P. Mori-Sánchez, J. Contreras-García, A. J. Cohen and W. Yang, *J. Am. Chem. Soc.*, 2010, **132**, 6498; (b) T. Lu and F. Chen, *J. Comput. Chem.*, 2012, **33**, 580.
- L. Pignataro, C. Bovio, M. Civera, U. Piarulli and C. Gennari, *Chem. – Eur. J.*, 2012, **18**, 10368.

